Biochemical and Biophysical Research Communications 424 (2012) 508–511

Contents lists available at SciVerse ScienceDirect

Biochemical and Biophysical Research Communications

journal homepage: www.elsevier.com/locate/ybbrc

Crystal structure of the rice branching enzyme I (BEI) in complex with maltopentaose

Kimiko Chaen [a], Junji Noguchi [a], Toshiro Omori [b], Yoshimitsu Kakuta [a,c], Makoto Kimura [a,c,*]

[a] Laboratory of Structural Biology, Graduate School of Systems Life Sciences, Kyushu University, Hakozaki 6-10-1, Fukuoka 812-8581, Japan
[b] Frontier Research Center, Sanwa Shurui Co. Ltd., 2231-1, Yamamoto, Usa Oita 879-0495, Japan
[c] Laboratory of Biochemistry, Department of Bioscience and Biotechnology, Graduate School, Faculty of Agriculture, Kyushu University, Hakozaki 6-10-1, Fukuoka 812-8581, Japan

ARTICLE INFO

Article history:
Received 15 June 2012
Available online 3 July 2012

Keywords:
Branching enzyme
Carbohydrate-binding module 48
Crystal structure
Glycoside hydrase family 13
Maltopentaose
Oryza sativa

ABSTRACT

Starch branching enzyme (SBE) catalyzes the cleavage of α-1,4-linkages and the subsequent transfer of α-1,4 glucan to form an α-1,6 branch point in amylopectin. We determined the crystal structure of the rice branching enzyme I (BEI) in complex with maltopentaose at a resolution of 2.2 Å. Maltopentaose bound to a hydrophobic pocket formed by the N-terminal helix, carbohydrate-binding module 48 (CBM48), and α-amylase domain. In addition, glucose moieties could be observed at molecular surfaces on the N-terminal helix (α2) and CBM48. Amino acid residues involved in the carbohydrate bindings are highly conserved in other SBEs, suggesting their generally conserved role in substrate binding for SBEs.

1. Introduction

Since starch branching enzyme (SBE) is the sole enzyme that catalyzes the formation of branch points by cleaving the α-1,4 linkage in polyglucans and reattaching the chain via an α-1,6 glucan linkage, the enzyme plays an important role in the biosynthesis of starch in plants. To date, a large number of SBEs have been identified in a variety of plants, including cereal endosperms, pea embryos, and potato tubers, and characterized in terms of biochemical and genetic properties [1 and references therein]. In rice endosperm, there are three isozymes of branching enzymes, BEI, BEIIa, and BEIIb, which are encoded by distinct genes [2 and references therein]. It is known that BEI and BEIIb are specifically expressed in the endosperm, while BEIIa is present in every [2] tissue, suggesting a distinct physiological role in rice. Satoh and co-workers isolated starch mutants of rice lacking three individual isozymes in the endosperm [3,4]. Biochemical analyses of deficient mutants revealed that a reduction in BEIIb leads to a specific decrease in short chains of degree of polymerization (DP) < 13, with the greatest decrease in chains of DP 8–11 [3], while a lack of BEI led to the synthesis of amylopectin containing fewer medium-sized (16 < DP < 23) and long (DP > 37) chains [4]. In contrast, the BEIIa-deficient mutant exhibited no significant change in the amylopectin chain. These results strongly suggest that BEI predominantly transfers less branched, longer chains with a DP greater than 10, whereas BEIIb preferentially transfers highly branched, shorter glucan chains with DP 3–9. Despite of a vast amount of biochemical data on the rice BEs, the molecular mechanism of catalysis and substrate recognition has remained unclear.

Previously, we overproduced BEI in *Escherichia coli* cells, and characterized the recombinant BEI with respect to biochemical properties [5] and crystal structure [6]. The sequence of the mature BEI (755 amino acids) indicated a modular architecture, consisting of carbohydrate binding module 48 (CBM48) (residues 59–160), the central $(\beta\alpha)_8$ catalytic module (residues 161–587), and an α-amylase C-domain (residues 588–702). Despite three modular structures, BEI is roughly ellipsoidal in shape with two globular domains that form a prominent groove which is proposed to serve as the α-polyglucan-binding site [6]. Amino acid residues Asp344 and Glu399, which are postulated to play an essential role in catalysis as a nucleophile and a general acid/base, respectively, are located at a central cleft in the groove [5,6]. To gain further insight into the structure–function relationship of BEI, we determined the crystal structure of BEI in complex with maltopentaose at a resolution of 2.2 Å with molecular replacement. The structure showed that carbohydrates bound to three molecular surfaces: maltopentaose bound to a hydrophobic pocket formed by the N-terminal helix, CBM48, and α-amylase domain, while glucose moieties could be localized at separate surfaces on the N-terminal helix (α2) and CBM48. Sequence comparison indicated that amino acid residues involved in the carbohydrate binding are highly conserved in other

* Corresponding author at: Laboratory of Biochemistry, Department of Bioscience and Biotechnology, Graduate School, Faculty of Agriculture, Kyushu University, Hakozaki 6-10-1, Fukuoka 812-8581, Japan. Fax: +81 92 642 2853.
E-mail address: mkimura@agr.kyushu-u.ac.jp (M. Kimura).

0006-291X/$ - see front matter © 2012 Elsevier Inc. All rights reserved.
http://dx.doi.org/10.1016/j.bbrc.2012.06.145

SBEs including isozymes, BEIIa and BEIIb. The present result provides an insight into the molecular determinants of α-glucan recognition by SBEs in general.

2. Materials and methods

2.1. Crystallization

Biochemical and structural studies suggested that Asp344 and Glu399 in BEI play an essential role in catalysis as a nucleophile and a general acid/base, respectively [5]. In the present study, the mutant referred to as E399Q, in which Glu399 was replaced by Gln, was prepared using site-directed mutagenesis kit, PrimeSTAR, and purified to homogeneity, as described for the wild-type BEI [5]. Subsequently, the core domain (pos. 1–702), referred to as E399Q$_{\Delta C}$, was prepared in the same manner as those described for BEI$_{\Delta C}$ [6]. E399Q$_{\Delta C}$ complexed with maltopentaose was crystallized using the sitting-drop vapor diffusion method under a protein solution (~2.5 mg/ml) containing 50 mM Tris–HCl (pH 8.0), 2% β-ME, and 300 mM maltopentaose. The E399Q$_{\Delta C}$-maltopentaose crystals were grown at 20 °C within two weeks against a reservoir containing 50 mM monopotassium phosphate (pH 5.0) and 12% PEG 3350.

2.2. Data collection and processing

Data collection of E399Q$_{\Delta C}$-maltopentaose was made using synchrotron radiation at beamline BL38B1 of SPring-8 (Harima, Japan), under cryogenic conditions with crystals soaked in a cryoprotectant solution containing 30% glycerol and cooled to 100 K in a nitrogen gas stream. The diffraction data were processed using HKL2000 [7].

2.3. Structure solution and refinement

The crystal structure of the E399Q$_{\Delta C}$-maltopentaose complex was solved by molecular replacement with the program Phaser [8] using the coordinates of BEI (PDB ID: 3AMK and 3AML) as a search model. An initial model was built using ARP/wARP [9] and Buccaneer [10] and a manual fitting to the electron density maps was performed using Coot [11]. The refinement procedures were carried out with REFMAC5 [12]. The stereochemical quality of the final model was assessed by PROCHECK [13]. The crystallographic parameters and final refinement statistics are summarized in Table 1. Figures were prepared using PyMol (http://www.pymol.sourceforge.net). The atomic coordinates of the E399Q$_{\Delta C}$-maltopentaose complex have been deposited in the Protein Data Bank with the accession code 3VU2.

3. Results and discussion

3.1. Structure determination

Crystal structure of E399QΔ_C, complexed with maltopentaose, was solved by molecular replacement using the coordinates of the BEI structures (PDB ID: 3AMK and 3AML) as search models and refined against 2.2 Å resolution. The space group of the crystal of the complex is $P2_1$ with two crystallographically independent complexes in an asymmetric unit. Two molecules in the asymmetric unit (referred to as MolA and MolB) have approximately identical conformation in terms of the overall fold of the proteins in the complex. The current model includes 693 of 702 amino acid residues for both MolA and MolB molecules, each having an R_{cryst} of 21.5% and R_{free} of 25.8% for data between a resolution of 50.0 and 2.2 Å. As the case for the BEIΔ_C structure, the first six N-terminal residues, three C-terminal residues, and loop regions between Gln469 and Gly473 and between Pro664 and Asn672 have week density. The model has geometries close to ideal with a rmsd of 0.008 Å and 1.1° from ideal values for bond lengths and angles, respectively. The stereochemistry of the final model was checked using the program PROCHECK [13], which indicated that 96.5% and 2.6% of the residues constituting BEI were in the most favored and allowed regions of the Ramachandran plot, respectively.

Table 1
Data collection and refinement statistics.

Data collection	Maltopeta complex
Space group	$P2_1$
Unit cell parameters	a = 73.81 Å, b = 66.56 Å, c = 169.63 Å, β = 89.97°
Beam line	SPring-8 BL38B1
Wavelength (Å)	1.000
Resolution range (Å)	50.0–2.20
Number of reflections	
Observed/Unique	266,977/72,156
Redundancy	3.7 (2.9)
R_{sym}[a]	0.070 (0.652)
$I/\sigma(I)$	22.1 (5.21)
Completeness (%)	88.5 (36.1)
Refinement statistics	
Resolution range (Å)	37.2–2.23
Number of reflections	
Working set/Test set	66,870/3653
Completeness (%)	87.8
R_{cryst}[b] (%)/R_{free}[c] (%)	21.5/25.8
Root mean square deviations	
Bond length (Å)/Bond angles (°)	0.008/1.1
Average B-factor (Å^2)/Number of atoms	
Protein	45.5/11,336
Maltopenta	58.7/112
Glucose	80.5/48
Glycerol	69.6/30
Water	44.3/787
Ramachandran analysis	
Most favored (%)	96.5
Allowed (%)	2.6
Disallowed (%)	0.9

Values in parentheses are for the highest-resolution shell.

[a] $R_{sym} = \sum(I - \langle I \rangle)/\sum\langle I \rangle$, where I is the intensity measurement for a given reflection and $\langle I \rangle$ is the average intensity for multiple measurements of this reflection.

[b] $R_{cryst} = \sum|F_{obs} - F_{cal}|/\sum F_{obs}$, where F_{obs} and F_{cal} are observed and calculated structure factor amplitudes.

[c] R_{free} value was calculated for R_{cryst}, using only an unrefined randomly chosen subset of reflection data (5%).

3.2. The overall structure of E399QΔ_C in complex with maltopentaose

The electron density maps of E399QΔ_C cocrystallized with maltopentaose revealed density for carbohydrates bound to each molecule MolA and MolB in an identical manner, allowing the modeling of maltopentaose at one site (referred to as site 1) and glucose at another sites referred to as site 2 and site 3. In the present structure, no electron density was observed at the central cleft in the groove which is proposed to serve as the α-polyglucan-binding site. Overall structure of the E399QΔ_C-maltopentaose complex is depicted in Fig. 1 and a detailed view on the coordination of carbohydrates on E399QΔ_C is presented in Fig. 2A–C. The maltopentaose binding pocket (site 1) is formed by the N-terminal helix (α2), a loop between β-strands β4 and β5 in CBM48, and α-helix (α6) in α-amylase domain (Fig. 2A). In the complex, the maltopentaose is fixed to the binding site *via* a sandwich-like stacking interaction between the hydrophobic side chains of Phe100 in CBM48 and

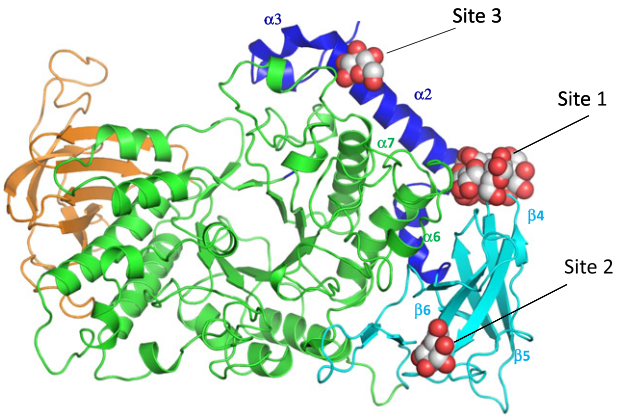

Fig. 1. Structure of the branching enzyme I (BEI) in complex with maltopentaose. The N-terminal helices are shown in blue, CBM48 in light blue, α-amylase domain in green, and α-amylase C domain in orange. Carbohydrates are drawn in space-filling form colored according to atom type with C gray and O red. The figure was drawn with PyMol (http://www.pymol.sourceforge.net). (For interpretation of the references to color in this figure legend, the reader is referred to the web version of this article.)

Trp319 in α-amylase domain. In addition, glucose units are firmly stabilized by an extensive network of hydrogen bonds. The side chains of His44 and Glu45 at the N-terminal helix (α2) interact with the second and third glucose units, respectively, and the side chain of Lys99 located at a loop between β-strands β4 and β5 in CBM48 interacts with terminal glucose, as shown in Fig. 2A. Furthermore, the side chains of His294, Glu295, Glu320, and Arg323 located at a loop between β-strand (β10) and α-helix (α6) in α-amylase domain interact with third and fourth glucose units.

In the binding sites 2 and 3, glucose moieties could be observed, being stabilized by stacking interactions between glucose units and the indole ring of Trp88 located on loops between β-strands β3 and β4 in CBM48 (site 2) and Tyr29 on the N-terminal helix (α2) (site 3) (Fig. 1B and C). Furthermore, hydrophobic side-chains of Leu370 and Val 374 located at a loop between β13 and α7 in α-amylase domain interact with glucose units at the binding site 3.

When we compared amino acid residues in the carbohydrate binding sites in BEI with corresponding residues in other SBEs including isozymes, BEIIa and BEIIb, they are highly conserved in all enzymes (Fig. 3). Particularly, the aromatic residues involved in the stacking interaction with glucose units are completely conserved in all SBEs. It is thus likely that the aromatic side-chains at the binding sites in BEI play a generally conserved role in substrate binding in SBEs.

3.3. Structural comparison of CBMs

The present structure indicates that CBM48 is principally responsible for carbohydrate binding for BEI. It is known that CMBs in carbohydrate-active enzymes exert their biological activity by maintaining the interaction of the enzyme with its insoluble substrates including granular starch [14]. Structural basis for the interaction between CBMs and carbohydrates has been extensively examined by biochemical and structural studies [15]. The best characterized CBM is the *Aspergillus niger* glucoamylase starch-binding domain, belonging to the CBM20 family [16]. The three-dimensional structure in complex with β-cyclodextrin was determined and the amino acid residues involved in the binding were well defined [16]. It was reported that there are two independent binding sites in CBM20 that are structurally and functionally different [16]. The interaction in the first site is proposed to act as the initial recognition site for starch, whereas the second site, which has stronger affinity to carbohydrate than the first site, is proposed to act as the more specific site which acts to lock CBM20 into place [15,16]. On the basis of the three-dimensional structure of the *A. niger* glucoamylase CBM20-β-cyclodextrin complex, a model structure was proposed that two starch strands are bound to the CBM20 in a perpendicular orientation, suggesting that either it may force starch strands apart thus increasing the hydrolysable surface or it may localize the enzyme to noncrystalline areas of starch [16].

Structural comparison of the BEI CBM48 with the *A. niger* glucoamylase CBM20 indicates that the sites 1 and 2 in BEI corresponds to the second binding site and the first binding site in the *A. niger* glucoamylase CBM20, respectively. In the E399QΔ_C-maltopentaose complex, a clear electron density was visible for maltopentaose at the site 1, while a week density corresponding to glucose could be observed at the site 2, as described above. This suggests the site 1 has a higher affinity to maltopentaose than the site 2 in BEI, which is consistent with the fact that the second binding sites in CBM20 has higher affinity to oligosaccharide than the first site [16]. Although BEI and glucoamylase have distinct catalytic reactions (transglycosylation and hydrolysis, respectively), the two oligosaccharide binding sites in BEI may play a role similar to those proposed for the *A. niger* glucoamylase CBM20. Alternatively, it could be tempting to speculate that the two binding sites observed in the present study might serve as a donor-strand and an acceptor-strand binding sites in BEI.

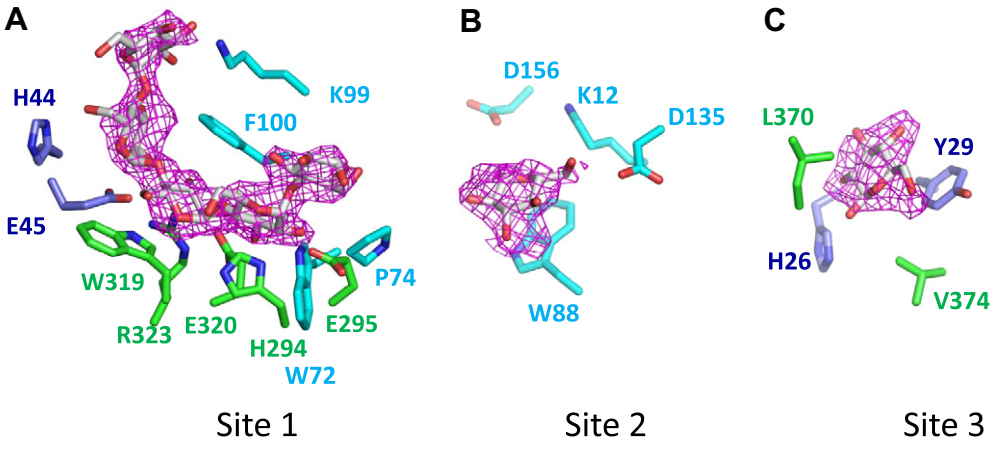

Fig. 2. Interactions observed in the crystal structure of the BEI–maltopentaose complex. The side-chains involved in the interactions with carbohydrates are colored as in Fig. 1. The simulated annealing omit maps contoured at 3.0σ, 2.5σ, and 4.0σ are drawn with maltopentaose at site 1 (A), glucose at site 2 (B), and glucose at site 3 (C) in red, respectively. (For interpretation of the references to color in this figure legend, the reader is referred to the web version of this article.)

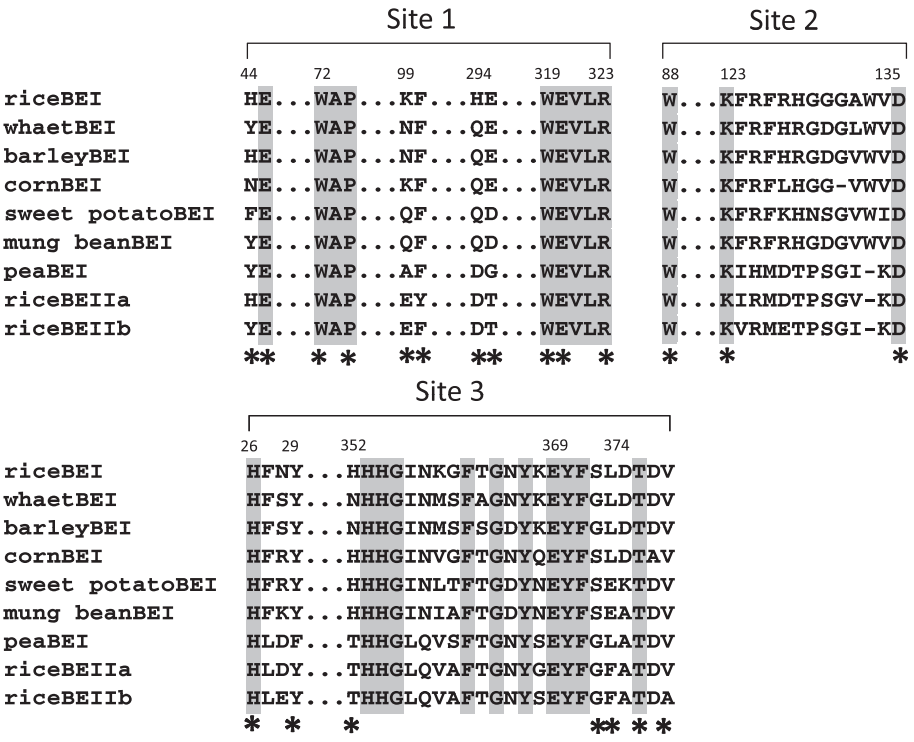

Fig. 3. Comparison of the amino acid residues involved in the carbohydrate binding of BEI with the corresponding residues in other BEs. The amino acid residues involved in the interaction with carbohydrates are indicated with asterisk and those conserved in BEs are shown in gray. The numbers at the top represent BEI numbering.

In the present structure analysis, despite that BEI was crystallized in the presence of a large molar excess of maltopentaose, no extra electron density could be observed at a prominent groove, which is proposed to serve as a substrate-binding site [6]. The BEI structure revealed that the extended loop structures in BEI narrow the putative substrate binding groove, as compared with the corresponding site in the *Klebsiella pnenmoniae* pullulanase [6]. It is thus conceivable that an authentic substrate-binding on the three carbohydrate binding sites observed in the present structure might cause a conformational change in the putative substrate-binding site. Further structural study of BEI in complex with longer oligosaccharides will provide an answer to this issue.

Acknowledgments

We thank the staff of Spring-8 and the Photon Factory for their assistance in collecting data. The synchrotron radiation experiments were performed at the BL38B1 of Spring-8 with the approval of the Japan Synchrotron Radiation Research Institute (JASRI) (Proposal No. 2007B1359 and 2007B1995), and Photon Factory. This study was supported in part by a grant from the Research for Promoting Technological Seeds program of Japan Science and Technology Agency (No. 15-020) and by a grant from the Iijima Kinen Foundation.

References

[1] J.S. Jeon, N. Ryoo, T.R. Hahn, H. Walia, Y. Nakamura, Starch biosynthesis in cereal endosperm, Plant Physiol. Biochem. 48 (2010) 383–392.
[2] Y. Nakamura, Y. Utsumi, T. Sawada, S. Aihara, C. Utsumi, M. Yoshida, S. Kitamura, Characterization of reactions of starch branching enzymes from rice endosperm, Plant Cell Physiol. 51 (2010) 776–794.
[3] A. Nishi, Y. Nakamura, N. Tanaka, H. Satoh, Biochemical and genetic analysis of the effects of amylase-extender mutation in rice endosperm, Plant Physiol. 127 (2001) 459–472.
[4] H. Satoh, A. Nishi, K. Yamashita, Y. Takemoto, Y. Tanaka, Y. Hosaka, A. Sakurai, N. Fujita, Y. Nakamura, Starch-branching enzyme I-deficient mutation specifically affects the structure and properties of starch in rice endosperm, Plant Physiol. 133 (2003) 1111–1121.
[5] N.T. Vu, H. Shimada, Y. Kakuta, T. Nakashima, H. Ida, T. Omori, A. Nishi, H. Satoh, M. Kimura, Biochemical and crystallographic characterization of the starch branching enzyme I (BEI) from *Oryza sativa* L., Biosci. Biotechnol. Biochem. 72 (2008) 2858–2866.
[6] J. Noguchi, K. Chaen, N.T. Vu, T. Akasaka, H. Shimada, T. Nakashima, A. Nishi, H. Satoh, T. Omori, Y. Kakuta, M. Kimura, Crystal structure of the branching enzyme I (BEI) from *Oryza sativa* L. with implications for catalysis and substrate binding, Glycobiology 21 (2011) 1108–1116.
[7] Z. Otwinowski, W. Minor, Processing of X-ray diffraction data collected in oscillation mode, Methods Enzymol. 276 (1997) 307–326.
[8] A.J. McCoy, R.W. Grosse-Kunstleve, P.D. Adams, M.D. Winn, L.C. Storoni, R.J. Read, Phaser crystallographic software, J. Appl. Crystallogr. 40 (2007) 658–674.
[9] R.J. Morris, A. Perrakis, V.S. Lamzin, ARP/wARP and automatic interpretation of protein electron density maps, Methods Enzymol. 374 (2003) 229–244.
[10] K. Cowtan, The Buccaneer software for automated model building. 1. Tracing protein chains, Acta Crystallogr. D: Biol. Crystallogr. 62 (2006) 1002–1011.
[11] P. Emsley, K. Cowtan, Coot: model-building tools for molecular graphics, Acta Crystallogr. D: Biol. Crystallogr. 60 (2004) 2126–2132.
[12] G.N. Murshudov, A.A. Vagin, E.J. Dodson, Refinement of macromolecular structures by the maximum-likelihood method, Acta Crystallogr. D: Biol. Crystallogr. 53 (1997) 240–255.
[13] R.A. Laskowski, M.W. MacArthur, D.S. Moss, J.M. Thornton, PROCHECK: a program to check the stereochemical quality of protein structures, J. Appl. Crystallogr. 26 (1993) 283–291.
[14] A.B. Boraston, D.N. Bolam, H.J. Gilbert, G.J. Davies, Carbohydrate-binding modules: fine-tuning polysaccharide recognition, Biochem. J. 382 (2004) 769–782.
[15] R. Rodriguez-Sanoja, N. Oviedo, S. Sanchez, Microbial starch-binding domain, Curr. Opin. Microbiol. 8 (2005) 260–267.
[16] K. Sorimachi, M.F.L. Gal-Coeffet, G. Williamson, D.B. Archer, M.P. Williamson, Solution structure of the granular starch binding domain of *Aspergillus niger* glucoamylase bound to beta-cyclodextrin, Structure 5 (1997) 647–661.